Journal of Materials Chemistry A

RSC Publishing

PAPER

View Article Online
View Journal | View Issue

Cite this: J. Mater. Chem. A, 2013, 1, 4577

Organophotocatalysis in nanostructured soft gel materials as tunable reaction vessels: comparison with homogeneous and micellar solutions†

Jürgen Bachl,[ab] Andreas Hohenleutner,[a] Basab Bijayi Dhar,[c] Carlos Cativiela,[b] Uday Maitra,[d] Burkhard König[a] and David Díaz Díaz*[ab]

Riboflavin tetraacetate-catalyzed aerobic photooxidation of 1-(4-methoxyphenyl)ethanol was investigated as a model reaction under blue visible light in different soft gel materials, aiming to establish their potential as reaction vessels for photochemical transformations. Three strategies involving different degrees of organization of the catalyst within the gel network were explored, and the results compared to those obtained in homogeneous and micellar solutions. In general, physical entrapment of both the catalyst and the substrate under optimized concentrations into several hydrogel matrices (including low-molecular-weight and biopolymer-based gels) allowed the photooxidation with conversions between 55 and 100% within 120 min (TOF $\sim$ 0.045–0.08 min^{-1}; $k_{obs} \sim$ 0.011–0.028 min^{-1}), albeit with first-order rates *ca.* 1–3-fold lower than in solution under comparable non-stirred conditions. Remarkably, the organogel made of a cyclohexane-based bisamide gelator in CH_3CN not only prevented the photodegradation of the catalyst but also afforded full conversion in less than 60 min (TOF $\sim$ 0.167 min^{-1}; $k_{obs} \sim$ 0.073 min^{-1}) without the need of additional proton transfer mediators (*e.g.*, thiourea) as it occurs in CH_3CN solutions. In general, the gelators could be recycled without detriment to their gelation ability and reaction rates. Moreover, kinetics could be fine-tuned according to the characteristics of the gel media. For instance, entangled fibrillar networks with relatively high mechanical strength were usually associated with lower reaction rates, whereas wrinkled laminated morphologies seemed to favor the reaction. In addition, the kinetics results showed in most cases a good correlation with the aeration efficiency of the gel media.

Received 15th November 2012
Accepted 1st February 2013

DOI: 10.1039/c3ta01109g

www.rsc.org/MaterialsA

1 Introduction

Inspired by nature, much effort has been devoted over the last decade to the study of meso-, micro- and nano-scale reactors. The main reason for this is the fact that many chemical reactions take place with high efficiency in natural confined environments where the motions of reactant molecules are restricted compared to those in free solution. Through biomimetic principles, a significant number of self-assembled and compartmentalized molecular (*e.g.*, micelles, vesicles, microemulsions, multilayered capsules, inorganic frameworks), macromolecular (*e.g.*, polymersomes, polymer micelles) and biomacromolecular (*e.g.*, viruses, protein cages) nanoreactors have been investigated in the context of chemical reactivity and highlighted in several excellent reviews.[1–9] Therein, numerous advantages have been attributed to the use of synthetic nanoreactors including, among others, the possibility of tailoring additional functionalities, organization and orientation of solvent, catalyst and reactant molecules, controllable molecular diffusion, large surface area to volume ratios and reduction of overheating/concentration effects. Thus, an improved control over the efficiency and selectivity of reactions carried out in constrained spaces compared to conventional solutions or heterogeneous media has been demonstrated in many of those examples. Nevertheless, predicting the outcome of a chemical process in a potential nanoreactor continues to be a scientific challenge mainly due to the number of thermodynamic and interfacial effects that should be considered and rationalized.[10]

Looking now at the plethora of chemical processes, photocatalysis constitutes undoubtedly a subject of increasing

[a]Institut für Organische Chemie, Universität Regensburg, Universitätsstr. 31, 93053 Regensburg, Germany. E-mail: David.Diaz@chemie.uni-regensburg.de; Fax: +49 941 9434121; Tel: +49 941 943 4681

[b]Instituto de Síntesis Química y Catálisis Homogénea (ISQCH), CSIC-Universidad de Zaragoza, Pedro Cerbuna 12, 50009 Zaragoza, Spain. E-mail: diazdiaz@unizar.es; Tel: +34 976 76 3496

[c]CReST, Chemical Engineering Division, National Chemical Laboratory, Dr Homi Bhabha Road, 411008 Pune, India

[d]Department of Organic Chemistry, Indian Institute of Science, 560012 Bangalore, India

† Electronic supplementary information (ESI) available: Synthesis and characterization of new compounds and materials, additional figures, tables and experimental details. See DOI: 10.1039/c3ta01109g

technological and economic importance owing to its critical role in many of today's energy and environmental concerns. Also here, the literature contains numerous investigations directed towards understanding photochemical processes in nanophotoreactors based on either porous inorganic structures or organized molecular assemblies (*e.g.*, titania spheres, lipid vesicles, foams, oil-in-water emulsions), which demonstrate the importance of these studies in the field of materials chemistry.[11] On the other hand, soft gel materials[12] have also been studied as structured reaction vessels and reusable catalysts,[13,14] although truly biomimetic catalysis[3] has not yet been demonstrated with these materials. In addition, the study of photochemical processes in gel media, involving embedded reactants that do not participate in the assembly of the viscoelastic network, has been scarcely explored.[13,15] In this sense, Bhat and Maitra published the most relevant study in 2007,[16] showing that the photodimerization of acenaphthylene occurs with higher *syn*/*anti* selectivity in bile acid-based hydrogels than in micellar solutions. Two years later, Shinkai and co-workers reported the selective photocyclodimerization of anthracene derivatives within an organogel matrix.[17] Eswaramoorthy, George and co-workers have demonstrated that clay–dye hybrid supramolecular hydrogels can act as efficient light-harvesting soft materials[18] to promote Förster resonant energy transfer.[19] Haldar and co-workers have also reported the successful formation of a charge-transfer complex between a tripeptide-based gelator and picric acid in gel phase.[20] Very recently, Biradha's group has described different effects of crystalline and gel states on the photodimerization of unsymmetrical olefins.[21] These few reports envisage the significant influence that the properties of the gel media and the local microenvironment may have on the outcome of a photochemical reaction.

From our point of view, the reduced number of photocatalytic studies on metal-free gels is rather surprising if we consider, for example, that hydrogels and natural cells (including those where light-driven reactions take place) have been found to share many features such as dynamic nature, water structuring, exclusion of solutes *via* phase-transition, physical consistency, multiple cooperative non-covalent interactions,[22] and therefore self-adaptivity.[23] Motivated by this paradigm and the appearance of new forms of gel bio-inspired materials with great potential for coacervate domains,[24] we aimed to gain insights into the impact of different gels on both the kinetics and selectivity of flavin-mediated aerobic photooxidation of benzyl alcohols as a model photocatalytic reaction. A comparative analysis was also made with the reaction performed in homogeneous and micellar systems.

2 Experimental section

2.1 Materials

Unless otherwise specified, all reagents, starting materials and solvents (p.a. grade) were purchased from commercial suppliers and used as received without further purification. See ESI† for detailed information about instrumentation, synthetic procedures, and characterization of compounds and materials.

2.2 Gelation experiments

In a typical gelation experiment (approach I), a weighed amount of all the required components (*i.e.*, gelator, substrate, and catalyst) and the appropriate solvent system (1 mL) were placed into a 4 mL screw-capped glass vial (4.5 cm length × 1.2 cm diameter) and heated gently with a heat gun until an isotropic solution was formed. In some cases, sonication of the mixture in an ultrasound bath for 30 s before heating allowed a faster dissolution of the solids. The resulting homogeneous solution was then allowed to slowly cool down to RT and left for at least 12 h to ensure equilibration. After this time, the so-formed soft materials were preliminarily classified as "gels" if they did not exhibit gravitational flow upon turning the vial upside down. The gel state was further confirmed by oscillatory rheological measurements. The gels were kept overnight in the dark for stabilization purposes before irradiation. Experimental details on other strategies (approaches II and III) are given in ESI.†

2.3 Typical procedures for catalytic photooxidation

Each experimental data point used for kinetics calculations represents the average value from at least two randomized measurements.

2.3.1 Representative reaction in homogeneous solutions. Riboflavin tetraacetate (**RFT**) (10.9 mg, 0.02 mmol) and 1-(4-methoxyphenyl)ethanol (**1**) (30.4 mg, 0.2 mmol) were placed into a conical flask and the mixture diluted with H_2O–DMSO or CH_3CN to reach a total volume of 40.0 mL containing 2% (v/v) DMSO. The mixture was stirred for 30 min in the dark to allow complete solubilization of both the catalyst and the substrate under aerobic conditions (without additional saturation with O_2).[25] Thiourea (0.5 mM) was used in some experiments as an electron-transfer mediator to enhance reaction rates in CH_3CN solutions (Table 1).[26] The homogeneous solution was split into several plastic-capped vials (4 cm length × 1.9 cm diameter; total volume of solution = 1 mL) equipped with a magnetic stirring bar. The reaction mixture was irradiated for the desired time under stirring (250 rpm) by means of a light-emitting diode (LED) (λ_{max} = 440 nm, 3 W). The vial was placed vertically above the aperture of the LED and the temperature of the mixture was held at 20 ± 1 °C during the experiments *via* a custom-made cooling apparatus (see ESI†). Work-up for reactions made in aqueous solutions: reaction mixtures were diluted with brine (5 mL) and extracted with CH_2Cl_2 (5 × 5 mL). The combined organic phases were dried over Na_2SO_4, filtered and the solvent was evaporated under reduced pressure (≤250 mbar). The obtained residue was redissolved in $CDCl_3$ (0.7 mL) for subsequent NMR analysis. Work-up for reactions performed in CH_3CN solutions: solvent was directly evaporated to dryness under reduced pressure and the residue redissolved in $CDCl_3$ (0.7 mL) for NMR analysis.

2.3.2 Representative reaction in micellar solutions. **RFT** (10.9 mg, 0.02 mmol), **1** (30.4 mg, 0.2 mmol) and sodium deoxycholate (**11**)[27] (199 mg, 480 μmol) were placed into a conical flask, diluted with H_2O (40.0 mL total volume) and the mixture stirred for 3 h in the dark to allow micelle formation and solubilization of both the catalyst and the substrate

Table 1 Kinetics parameters of **RFT**-catalyzed photooxidation of **1** in homogeneous and micellar solutions, and the effect of stirring[a]

Entry	Solvent system[b]	[Substrate] (mmol L^{-1})	[Catalyst] (mol%)	[**TU**] (mmol L^{-1})	[**NaDC**] (mmol L^{-1})	Irradiation time (min)	Conversion (%)[e]	TON	TOF (min^{-1})	Rate constant, k_{obs} ($\times 10^{-3}$ min^{-1})	Half-life, $t_{1/2}$ (min^{-1})
1	H_2O–DMSO[c]	5	10	—	—	30	100	10.0	0.33	154.2 ± 7.71	4.5 ± 0.21
2	H_2O–DMSO[c,d]	5	10	—	—	90	100	10.0	0.11	37.3 ± 0.78	18.6 ± 0.38
3	CH_3CN	5	10	—	—	240	25	2.5	0.01	1.3 ± 0.07	533.2 ± 2.86
4	CH_3CN	5	10	0.5	—	120	69	6.9	0.06	15.5 ± 0.57	44.7 ± 1.59
5	CH_3CN[d]	5	10	0.5	—	240	43	4.3	0.02	2.6 ± 0.07	266.6 ± 6.99
6	H_2O	5	10	—	12.0	20	100	10.0	0.50	251.9 ± 9.33	2.8 ± 0.10
7	H_2O[d]	5	10	—	12.0	90	100	10.0	0.11	60.6 ± 3.47	11.4 ± 0.62

[a] *Reaction conditions*: $T = 20 \pm 1$ °C; light source = LED blue visible light ($\lambda_{max} = 440$ nm, 3 W); stirring at 250 rpm unless otherwise indicated. Abbreviations: **RFT** = riboflavin tetraacetate; **TU** = thiourea; **NaDC** = sodium deoxycholate = **11**; TON = turnover number (catalyst productivity); TOF = turnover frequency (catalyst activity). Square brackets refer to concentration. [b] Total solvent volume = 1 mL. [c] 2% (v/v) DMSO was necessary here for complete solubilization of all components. [d] Reactions carried out without stirring. [e] Reaction conversion over time for kinetics calculations was determined by ^{1}H NMR analysis. Estimated error = ±1.5%. For additional catalyst/substrate molar ratios, see ESI.

(resulting concentrations in the micellar solution: **11** = 12.0 mM, **RFT** = 0.5 mM, **1** = 5 mM). The homogeneous solution was then split into several sample vials (4 cm length × 1.9 cm diameter; total volume of solution = 1 mL) and subjected to LED irradiation ($\lambda_{max} = 440$ nm, 3 W) under stirring at 20 ± 1 °C (see ESI†). After irradiation, the samples were diluted with brine (5 mL), and extracted with CH_2Cl_2 (5 × 5 mL). The combined organic phases were dried over Na_2SO_4, filtered, and concentrated. The obtained residue was redissolved in $CDCl_3$ (0.7 mL) for NMR analysis or in iPrOH (1 mL) for HPLC-analysis after filtration through a PTFE filter.

2.3.3 Representative reaction in gel media. **RFT** (50 μL from a 0.01 M solution in CH_2Cl_2) and **1** (50 μL from a 0.1 M solution in CH_2Cl_2) were added to a 5 mL sample vial (4 cm height × 1.9 cm diameter) containing the specified amount of the respective gelator. The solvent was then allowed to slowly evaporate, and the mixture diluted with the appropriate solvent system for gelation (1 mL). The gels were prepared as described above. Alternatively, the gelator was weighed into a vial and **1** (50 μL from a 0.1 M solution in CH_2Cl_2) was added. After evaporation of the solvent, resuspension of the mixture and gel formation, **RFT** (50 μL from a 0.1 M solution in CH_2Cl_2) was carefully added on top of the gel and allowed to diffuse overnight. After an equilibration period (12 h), the samples were subjected to LED irradiation ($\lambda_{max} = 440$ nm, 3 W) at 20 ± 1 °C (see ESI†). For kinetics calculations, irradiation was stopped after a certain time and the gels dissolved by dilution, heating, and mechanical agitation. The solutions of the destroyed gels were extracted with CH_2Cl_2 (5 × 5 mL). The combined organic phases were dried over Na_2SO_4, filtered, and evaporated. The residue was redissolved in $CDCl_3$ for NMR analysis or in iPrOH for HPLC-analysis as described for micellar systems.[28]

3 Results and discussion

Flavin cofactors such as riboflavin (vitamin B2), flavin adenine mononucleotide (FMN), and flavin adenine dinucleotide (FAD) are well known as versatile catalysts in both one-electron and two-electron redox processes, playing a key role in a number of light-regulated biological processes.[29] Moreover, riboflavin-based organocatalysis has recently gained much attention as a green and economic alternative to the corresponding metal-catalyzed reactions.[30–33] For this investigation, we selected 1-(4-methoxyphenyl)ethanol (**1**) as a model activated substrate to study its photoinduced oxidation in different media upon irradiation with blue visible light ($\lambda_{max} = 440$ nm) in the presence of **RFT** as a non-toxic photocatalyst and aerial O_2 as a terminal oxidant (Scheme 1). As it occurs with other flavin-derivatives, **RFT**-mediated photooxidation of benzyl alcohols[25,26,34–38] takes advantage of the increased oxidation power of the chromophore in its oxidized state ($\mathbf{RFT_{ox}}$) upon excitation by visible light.[25] In the presence of an electron-donor (*e.g.*, benzyl alcohol), triplet-excited $\mathbf{RFT_{ox}}$ undergoes a subsequent two-electron reduction and protonation to generate the corresponding dihydroflavin ($\mathbf{RFT_{red}}$). Finally, $\mathbf{RFT_{red}}$ is rapidly and stoichiometrically reoxidized to $\mathbf{RFT_{ox}}$ by aerial O_2, yielding H_2O_2 as the sole byproduct.[39]

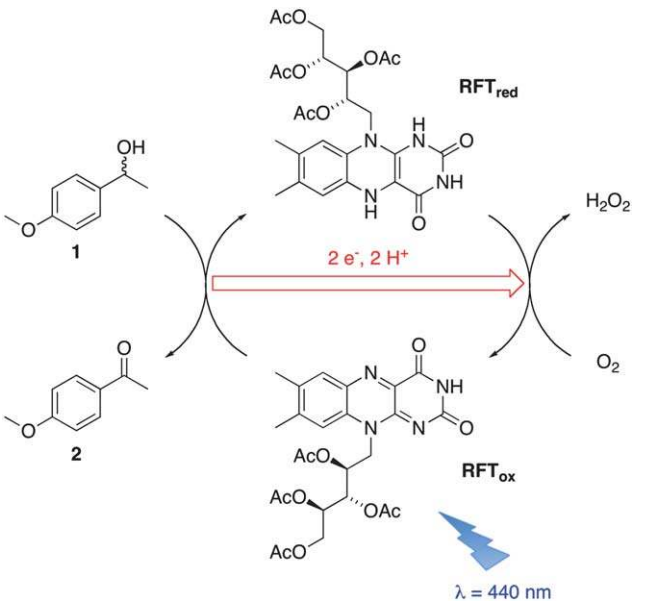

Scheme 1 Catalytic cycle of aerobic photooxidation of **1** under blue visible light catalyzed by **RFT**.

In order to draw meaningful comparisons, the reaction kinetics was first studied in homogeneous and micellar solutions as a reference scenario, and subsequently in several gel systems including those made from low-molecular-weight (LMW) and biopolymer-based gelators. Both aqueous and organic environments were also considered in this investigation. All reactions were performed under aerobic conditions using commercially available LEDs with emission maximum centered at $\lambda_{max} = 440$ nm as the light source, which corresponds roughly to the longest wavelength absorption maximum of $\mathbf{RFT_{ox}}$.

3.1 Photooxidation in homogeneous and micellar solutions

For comparative purposes, the maximum catalyst loading (*i.e.*, 10 mol%) in these experiments was chosen based on the ability of the gel systems to integrate the catalyst without major disruption of the fibrillar gel network (*vide infra*). Under these conditions, the kinetics of the reaction was studied in both aqueous and CH_3CN solutions (Table 1, entries 1–5).[28] Apparent first order rate constants (k_{obs}) were estimated from the slopes of ln[**1**] against time plots.[40] In agreement with previous observations made by some of us,[25,26] almost complete conversion of **1** into ketone **2** upon irradiation with blue visible light was achieved without formation of byproducts[41] within 30 min in aqueous stirred solution, whereas only 5% conversion was reached in CH_3CN after the same reaction time.[28] Thus, the catalyst activity (average TOF) was 33-fold higher in aqueous than in CH_3CN solution under comparable conditions (Table 1, entry 1 *vs.* 3). As expected, the addition of thiourea (0.5 mM) as a proton transfer mediator for the first reaction step caused a remarkable enhancement of the photooxidation rate in CH_3CN by a factor of *ca.* **12** under the conditions described in Table 1 (entry 3 *vs.* 4), although catalyst deactivation was observed after 40 min (*ca.* 50% conversion).[25,26]

On the other hand, previous investigations have demonstrated that performing photochemical reactions in the presence of bile salt micelles could significantly alter their course and selectivity.[42,43] For this reason, and considering the wide use of bile salts also as LMW gelators,[44] we additionally performed the above reaction as comparative control in micellar solutions of sodium deoxycholate (**NaDC**) (Table 1, entries 6 and 7). Micellar medium was prepared by adjusting the concentration of **NaDC** to 12 mM as previously described.[27] In this case, the micellar medium allowed complete solubilization of both the substrate and the catalyst without the need of organic co-solvents like DMSO, achieving quantitative conversion within 20 min under stirring conditions. Thus, the micellar medium caused a modest enhancement of the rate constant (*ca.* 1.6-fold increase) in comparison with that in H_2O–DMSO solution.

Nevertheless, it is important to remark that the catalyst activity in the above media underwent a 3–6-fold drop when carried out without moderate stirring (Table 1, entries 2, 5 and 7), which is in good agreement with previous observations[25] and suggests the existence of non-homogeneous microphases and a more complex nature of the kinetics. Moreover, HPLC analysis of the reaction mixture showed that the chiral microenvironment provided by **NaDC** did not induce any enantioselective oxidation of (±) **1**.[28]

3.2 Photooxidation in gel media

In principle, we could expect both diffusion-controlled and electron-transfer processes to be altered within viscoelastic gels due to constrained molecular mobility and light scattering phenomena.[45] However, among a number of potential advantages of gel materials as reaction vessels,[13] their two-phase nature and highly solvated 3D-network could facilitate the separation of catalysts and products, provide a much higher accessibility of small reactants in comparison with other heterogeneous catalysts, and/or promote different orientations of the chromophore.

In this work, we considered three different strategies in order to assess the actual potential of nanostructured soft gel materials as tunable reaction vessels for the **RFT**-catalyzed photooxidation of **1** under irradiation with blue visible light: use of systems with the photocatalyst physically entrapped into the gel matrices (approach I); systems where the photocatalyst is covalently attached to a complementary gelator structure (approach II); and bicomponent gelator systems, in which one of the complementary partners needed for building the 3D gel network acts as the photocatalyst (approach III).

• Approach I: For this strategy we considered a number of known bio-based polymers (*i.e.*, Fig. 1: methylcellulose (**3**), κ-carrageenan (**4**), gelatin (**5**)), and LMW gelators (*i.e.*, Fig. 1: compounds **6–12**) with distinctive properties in order to evaluate their possible effects on both selectivity and reaction kinetics. In the case of **NaDC** (**11**), the micellar concentration was *ca.* 4-fold increased to reach the minimum gelation concentration (MGC, 48.25 mM). All compounds could form stable hydrogels under different conditions, except bisamide **7** that was selected as a versatile organogelator for comparison with the less efficient reaction in CH_3CN solutions. Moreover, chiral hydrogelators were selected in order to also investigate any possible enantioselective recognition of the racemic substrate enabled by attractive forces with the self-assembled fibers. Such possible interactions[46] may provide regions of lower polarity within a chiral environment, in which photosensitizers and/or substrates with moderate water-solubility could be preorganized in a selective manner.[47–49] In principle, a similar reasoning could also be made for approaches II and III.

Initially, a series of experiments were necessary to define the conditions (*e.g.*, concentration of components, solvent system) to entrap both the catalyst and the substrate into the gel matrices without causing major disruption of their microstructure and viscoelastic properties. As shown in Fig. 2, the relative opacity of the pure gels was also preserved upon incorporation of **RFT** and **1**. In general, the opacity of the materials made from gelators **7–10** suggested the formation of aggregates smaller than the visible wavelength range.

The use of a custom-made cooling apparatus (see ESI†) was especially important for the kinetics experiments under LED irradiation ($\lambda_{max} = 440$ nm, 3 W). Thus, a constant reaction

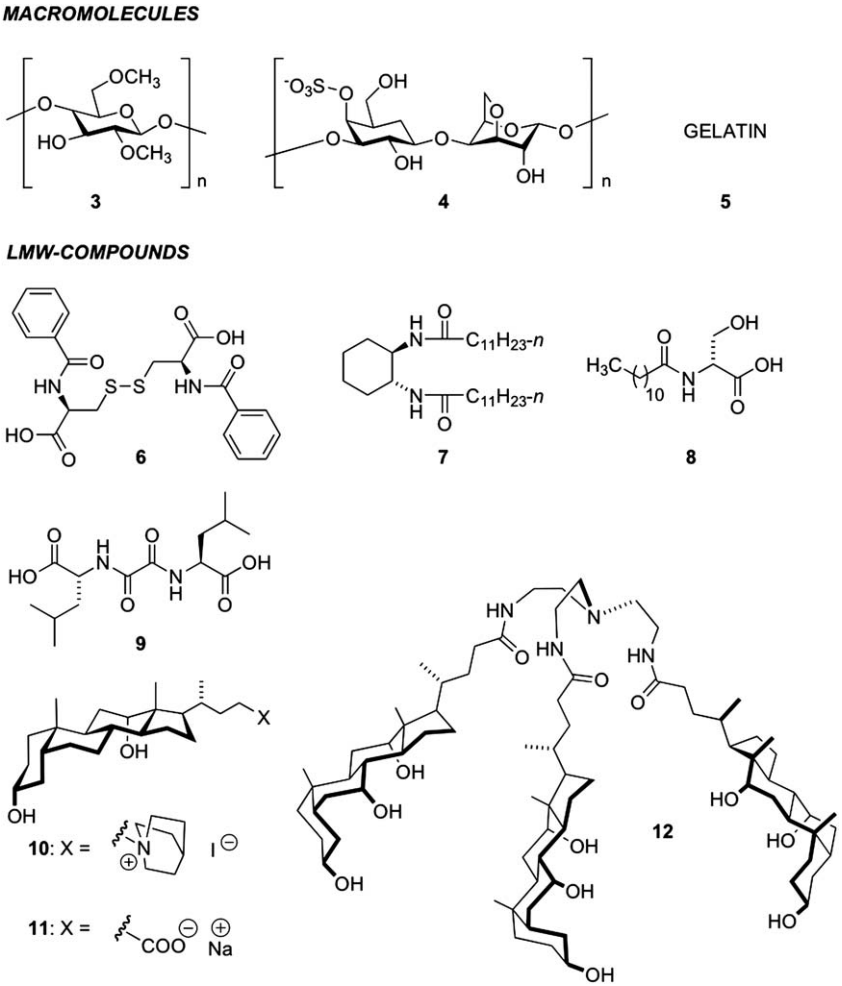

Fig. 1 Library of structurally diverse gelators used to study **RFT**-catalyzed photooxidation of **1** in gel media (approach I).

temperature far below the *gel*-to-*sol* phase transition temperatures (T_{gel}) was ensured to prevent disruption of the organized self-assembled fibrillar networks by a thermal shock and further melting of the gels. The stability of the bulk materials upon doping and irradiation was confirmed by the absence of a visible liquid phase, as well as FT-IR analyses before and after irradiation. In general, the spectra showed no significant modification of the H-bonding pattern (*e.g.*, amide I at ν = 1638–1740 cm^{-1}, amide II at ν = 1525–1635 cm^{-1}, H-bound OH stretching at ν = 3315–3335 cm^{-1}) after doping the materials (under optimized concentrations), and during irradiation.[28] Furthermore, the absorption properties of **RFT** were in general maintained upon incorporation into the gel matrices as demonstrated by UV-vis spectroscopy.[28] Minor disruption of the nanostructures was also confirmed by electron microscopy imaging (*vide infra*).[28]

We were delighted to observe that **RFT**-catalyzed photooxidation of **1** proceeded, under the above conditions, with conversions in the 23–100% range (Table 2). Regardless of the reaction media, control experiments carried out in the absence of **RFT** or light irradiation (λ_{max} = 440 nm) showed no conversion of substrate **1**. In addition, quantitative analysis of different sections of gel samples demonstrated a reasonably homogeneous distribution of the reaction product, which was in agreement with the intrinsic dynamic nature of the gels and a relatively uniform irradiation along the bulk materials.[28] However, it should be noted that the potential gradient of light intensity in the case of larger reaction volumes could influence catalyst activation. As expected for diffusion-controlled processes, photooxidation rates of **1** in hydrogel media were on average 10–20-fold lower than those in stirred solution, but only 1–3-fold lower under non-stirred conditions, which represents to some extent a more similar scenario to the reactions inside the gels.

Only hydrogels made of bile salt-based gelator **10** in 0.5 M NaCl (Table 2, entry 9) were inefficient as reaction vessels (*i.e.*, conversion < 5%), probably due to the sensitivity of the excimer fluorescence towards microenvironmental changes. On the other hand, one of the most surprising and interesting results was the rapid reaction observed in the organogel made of bisamide gelator **7** in CH_3CN (Table 2, entry 6). In contrast to the reaction carried out in CH_3CN solution, the gel environment not only prevented deactivation of the catalyst, but also afforded full conversion in less than 60 min without the need of thiourea

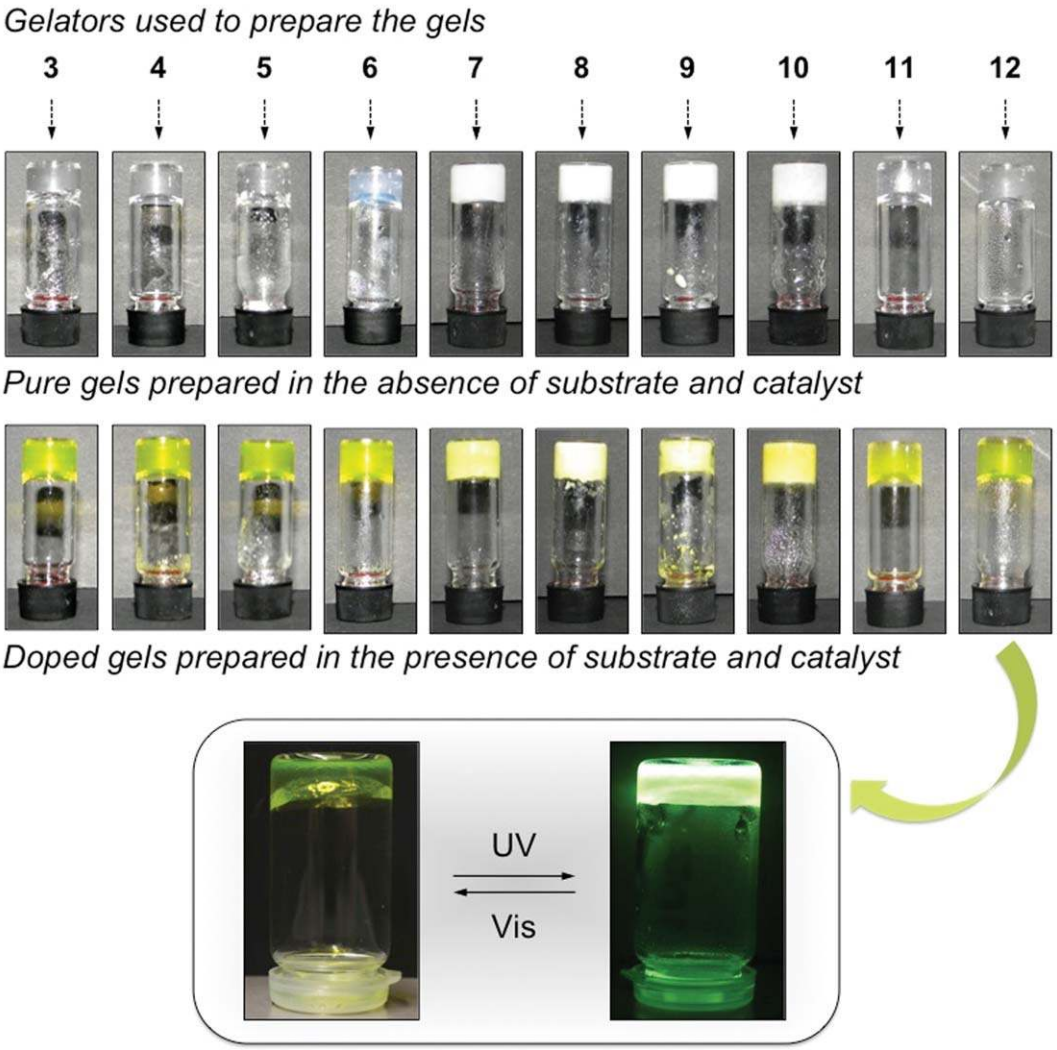

Fig. 2 Photographs of upside-down vials containing stable gels prepared with each gelator (*i.e.*, **3–12**) at a given concentration (see Table 2) in the absence and presence of substrate **1** (5 mM) and the **RFT** catalyst (10 mol%) using 1 mL of solvent (optimized conditions). The bright yellow color is derived from the catalyst. Solvent used in each case: [**3–5**, **8–9**] = H_2O; [**6**] = H_2O–DMSO (95/5 v/v); [**7**] = CH_3CN; [**10**] = 0.5 M NaCl; [**11**] = phosphate buffer; [**12**] = H_2O–AcOH (80/20 v/v). Note that compounds **6**, **10**, **11** and **12** did not form stable hydrogels in pure water. Bottom: example of a fluorescent hydrogel made of **12** under visible and UV-light.

and stirring. This result suggests the existence of favorable interactions between gel fibers and the substrate and/or catalyst, and will constitute the focus of a further detailed study. A potential role of secondary amides as proton transfer mediators, similar to thiourea, in solvents like CH_3CN[26] was disproved in control experiments.[28]

As it occurs in solution, some of the doped gels showed significant bleaching during irradiation at $\lambda_{max} = 440$ nm due to photodegradation of the **RFT** catalyst.[50] In the case of translucent gels, such a process could be easily confirmed by UV-vis spectroscopy (Fig. 3). Visual monitoring of the degree of bleaching during the experiments was in good agreement with the decrease in the reaction rate and stagnation of the process after a certain irradiation time.[28]

It is also worth mentioning that both LMW and polymer gelators could be easily recovered (*i.e.*, 92–98% of the original weight) after the photochemical reaction and reused for further experiments without any appreciable deterioration of the gelation ability and photoconversion rates. The purity of recycled materials was confirmed by ^{1}H NMR spectroscopy. In general, recycling experiments in the case of hydrogels involved lyophilization, liquid–solid extraction of the corresponding xerogels, and drying under vacuum. In the case of organogels, the first two steps were replaced by solvent evaporation and subsequent recrystallization of the gelator.[28] On the other hand, it should be considered that, in contrast to other immobilized flavins,[25] the use of doped photoluminescent xerogels (produced from the corresponding doped gels by the freeze-drying method) is not appropriate for the purposes of this work due to visible leaching of the **RFT** catalyst when swollen in aqueous or organic solutions (even under non-stirred conditions), and in sufficient amounts to catalyze the reaction.[28]

• Approach II: In order to gain additional insights into the effects of the gel-like microenvironment of the chromophore on

Table 2 Kinetics parameters of **RFT**-catalyzed photooxidation of **1** in different gel media under optimized conditions[a]

Entry	Gelator system	Solvent system[b]	[Gelator] (% w/v)	[Substrate] (mmol L^{-1})	[Catalyst] (mol%)	Irradiation time (min)	Conversion (%)[c]	TON	TOF ($\times 10^{-2}$ min^{-1})	Rate constant k_{obs} ($\times 10^{-3}$ min^{-1})	Half-life, $t_{1/2}$ (min^{-1})
1	**3**	H_2O	5.0	5	10	120	83	8.3	6.9	17.3 ± 0.07	40.1 ± 0.16
2	**4**	H_2O	2.0	5	10	120	90	9.0	7.5	20.8 ± 0.49	33.3 ± 0.78
3	**3** + **4**[d]	H_2O	2.0	5	10	120	96	9.6	8.0	28.2 ± 2.76	24.6 ± 2.19
4	**5**	H_2O	1.5	5	10	120	76	7.6	6.3	12.3 ± 0.42	56.4 ± 1.86
5	**6**	H_2O–DMSO[g]	0.3	5	10	120	23	2.3	1.9	2.7 ± 0.21	256.7 ± 18.53
6	**7**	CH_3CN	0.5	5	10	60	100	10.0	16.7	72.6 ± 8.34	9.6 ± 0.98
7	**8**	H_2O	3.0	5	10	120	70	7.0	5.8	11.0 ± 0.07	63.0 ± 0.40
8	**9**	H_2O	3.0	5	10	120	69	6.9	5.8	11.5 ± 0.57	60.3 ± 2.85
9	**10**	0.5 M NaCl[h]	2.0	5	10	360	14	1.4	0.4	0.5 ± 0.07	1386.3 ± 19.14
10	**11**	PBS[i]	2.0	5	10	120	55	5.5	4.6	19.3 ± 3.18	35.9 ± 5.08
11	**12**	H_2O–AcOH[j]	2.0	5	10	120	100	10.0	8.3	19.7 ± 0.64	35.2 ± 1.11
12	**15** + **11**[e]	PBS[i]	2.0	5	10	120	54	5.4	4.5	18.7 ± 0.07	37.1 ± 0.14
13	**RFT** + **16**[f]	H_2O	3.5	5	10	480	63	6.3	1.3	13.5 ± 1.48	51.3 ± 5.07

[a] *Reaction conditions*: $T = 20 \pm 1$ °C; light source = LED blue visible light (λ_{max} = 440 nm, 3 W). Abbreviations: **RFT** = riboflavin tetraacetate; TON = turnover number (catalyst productivity); TOF = turnover frequency (catalyst activity). Square brackets refer to concentration. [b] Total solvent volume = 1 mL. [c] Reaction conversion over time for kinetics calculations was determined by ^{1}H NMR analysis. Estimated error = ±1.5%. [d] Weight ratio = 1 : 1. [e] Molar ratio of gelator system [**15** : **11**] = 1 : 96.5. [f] Molar ratio of gelator system [**RFT** : **16**] = 1 : 1. [g] Volume ratio = 95/5. [h] Although these gels could also be formed in the presence of up to 20% of organic solvents such as MeOH or DMSO, no enhancement of the conversion was observed. [i] Phosphate buffer solution, pH 7.5. [j] Volume ratio = 80/20.

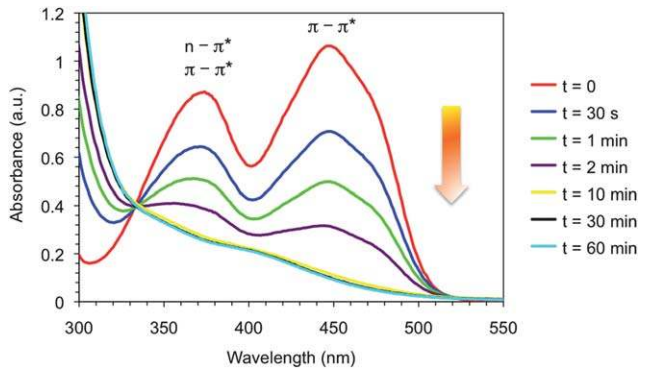

Fig. 3 Evolution of the UV-vis spectrum of the doped gel made from gelator **3** during irradiation with LED blue visible light (λ_{max} = 440 nm, 3 W). Signals at λ_{max} = 373 and 445 nm are characteristic of the **RFT** catalyst. Note that time values in the spectra do not correlate to real bleaching rates observed during kinetics experiments due to different light pathways. For additional details and examples, see ESI.†

the catalytic activity, we also explored a second strategy based on flavin-based catalysts covalently tethered to a complementary gelator structure. In principle, such systems may provide a different catalyst–gel network interface compared to the previous non-covalent approach, which could have an impact on the catalytic process.

Herein, we synthesized conjugate **15** by EDC-coupling of cholic acid (**13**) and flavin derivative **14** bearing an ethylene linker with a primary amine (Fig. 4). Although **15** did not present gelation ability, its design allowed further co-assembly with structurally related gelator **11** (sodium deoxycholate) under adequate concentrations in order to obtain stable hydrogels. UV-vis and fluorescence spectra of this hybrid showed no shift of the characteristic absorption and emission bands, respectively, in comparison with the solution state. In terms of scope, this behavior was also found with alternative conjugates (*e.g.*, [**15** + **12**]).[28] Therefore, although no firm conclusions could be drawn regarding the hydrophobicity of the chromophore environment in the gel matrix, preservation of the spectroscopic properties made this type of hydrogel also suitable as a reaction vessel for testing the photooxidation of **1**. However, at least in our case, the expected better organization of the catalyst within the gel network defined by gelator **11** did not show a significant effect on the photooxidation rate (Table 2, entry 12 *vs.* 10).

• Approach III: Finally, photooxidation of **1** was also studied using gel-based materials in which the flavin-based catalyst formed part, an indispensable component, of the supramolecular gel network. This approach was inspired by a recent report

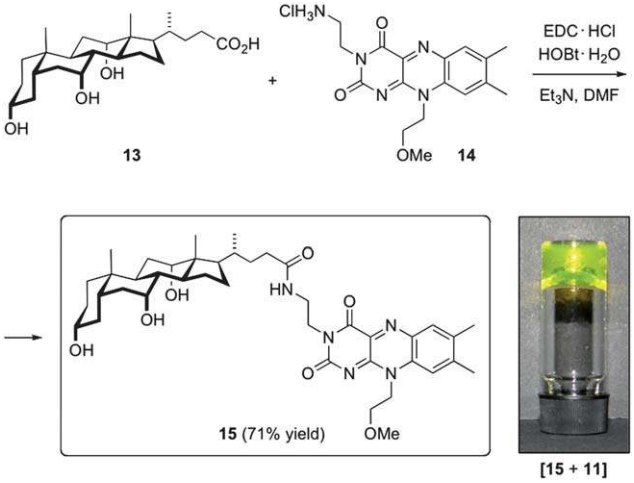

Fig. 4 Synthesis of catalyst **15** and hydrogel formation upon being co-assembled with gelator **11** (approach II). Substrate **1** was incorporated into the gel for comparative kinetics experiments as described in Table 2.

from Nandi and co-workers, in which the formation of a highly fluorescent H-bonded complex between riboflavin and 6-methyl-1,3,5-triazine-2,4-diamine (**16**) (1 : 1 molar ratio) was described to prepare a stable hydrogel.[51] We found that riboflavin could also be exchanged by **RFT** (Fig. 5) to form an analogous hydrogel, which was more appropriate as a model medium for our studies. Interestingly, the use of **RFT** instead of riboflavin allowed the formation of hydrogels with higher thermal–mechanical stability, and without significant bleaching even after 2 h of irradiation.[28] In general, the results obtained with this system (Table 2, entry 13), even at much higher catalyst loading, showed *ca.* 4–6-fold reduction of the catalyst activity in comparison with the values obtained using approach I.[28]

Thus, the degree of participation of the photocatalyst in the construction of the gel network was inversely correlated to its catalytic activity. Kinetics studies revealed a lower reaction conversion even under 4-fold increased irradiation times (*i.e.*, 63% conversion after 480 min), which could be explained by unfavorable substrate–catalyst interactions, significant restricted diffusion of reagents and/or hindered excimer formation.

Control experiments were performed with related hydrogels made of riboflavin or **RFT** and salicylic acid instead of acetoguanamine. In these cases, the different H-bonding moieties caused quenching of photoluminescence due to a less efficient formation of a hydrophobic core based on π-stacking interactions, which seems to be responsible for the stabilization of the excited state by resonance.[51] As a consequence, the photooxidation of **1** was completely inhibited in these hydrogels,[28] pointing out the importance of the specific H-bonding pattern (involving the isoalloxazine moiety of the riboflavin catalyst) in this approach.

A comparative analysis of the first-order kinetics plots[28] (Fig. 6) clearly demonstrated the possibility of fine-tuning the photooxidation kinetics (*i.e.*, k_{obs} range ~ 0.005–0.073 min^{-1}) depending on the characteristics of the gel media (see the next section for an extended discussion). In addition, it should be noted that both substrate enantiomers were equally photooxidized, as confirmed by HPLC,[28] in all gel media tested in this work. This result suggests the absence of favored hydrophobic interactions between one specific enantiomer and the corresponding gel network.

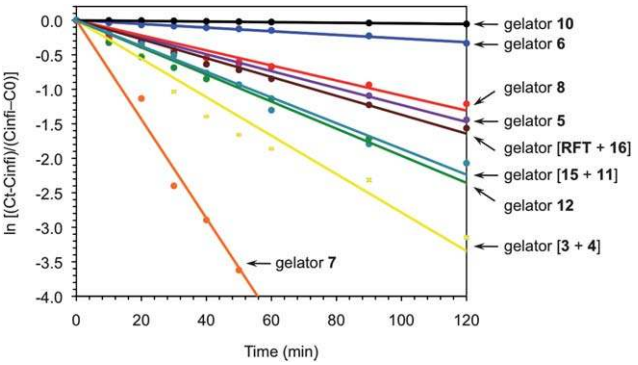

Fig. 6 First-order kinetics plots of **RFT**-catalyzed photooxidation of **1** in different gel media according to selected entries in Table 2. Each data point represents the average of two independent measurements. Abbreviations: C_{infi} = final concentration, at infinite time; C_t = concentration at a given time t; C_0 = initial concentration, at time t = zero.

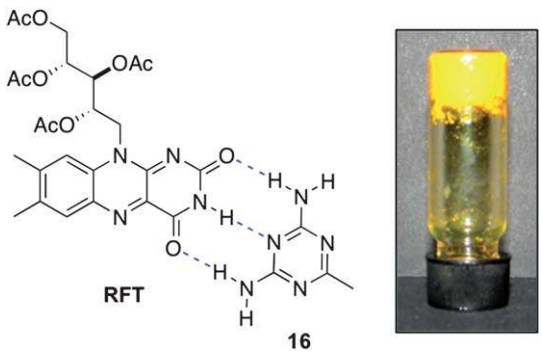

Fig. 5 Bicomponent supramolecular hydrogel made of an equimolar mixture of **RFT** and **16** (approach III). Substrate **1** was incorporated into the gel for comparative kinetics experiments as described in Table 2.

3.2.1 Gel properties and relationships with kinetics. Mechanical, thermal, morphological and aeration efficiency of all gels were studied as part of their characterization, and to identify any underlying connection with the reaction kinetics (Table 3). Thus, oscillatory rheological experiments confirmed the viscoelastic nature of all systems, showing an average storage modulus (G') with low dependence on the frequency (*i.e.*, $G' \sim \omega^{0.01-0.06}$), and at least one order of magnitude higher than the loss modulus (G'') within the linear regime.[28] The higher internal resistance was observed for some biopolymer-based hydrogels (Table 3, entries 2 and 4 ⇒ gelators **4** and **5**) according to the lower loss factors (tan $\delta \leq 0.1$). Interestingly, similar damping properties were also found for the bicomponent supramolecular hydrogel (Table 3, entry 13 ⇒ gelator [**RTF** + **16**]), whereas other LMW hydrogels were slightly weaker (Table 3, entries 5, 8, and 9 ⇒ gelators **6**, **9**, and **10**). In contrast, methylcellulose and some bile acid and serine based LMW gelators (Table 3, entries 1, 7, 10, and 11 ⇒ gelators **3**, **8**, **11**, and **12**) presented poorer mechanical strength.

In general, the same tendency was observed after incorporation of reagents (under optimized concentrations) into the gel matrices, albeit with a certain detriment to the thermal stability. For instance, the decrease in the T_{gel} value upon doping was in general relatively small ($\Delta T_{gel} \sim 5$–15%) suggesting preservation of the global gel structure, which was further confirmed by field emission electron scanning microscopy (FESEM).[28] The only exception was found with the hydrogel made of cystine-based gelator **6** ($\Delta T_{gel} \sim 42\%$), which was also found useless as a reaction vessel. If necessary, a possible way to compensate the thermal destabilization of the gels after doping would be to enhance the gelator concentration, which in some cases could be 4-fold increased without causing major changes in the rate constants.

Fig. 7 provides some insights into the microstructure of the different gel systems. Interestingly, well-defined and entangled

Published on 01 February 2013 on http://pubs.rsc.org | doi:10.1039/C3TA01109G

Table 3 Representative thermo-mechanical properties and aeration efficiency of gels used as reaction vessels for **RFT**-catalyzed photooxidation of **1**[a]

Entry	Gelator system	Solvent system	Storage modulus G' (Pa)[b]	Loss modulus G'' (Pa)[b]	Loss factor tan δ	T_{gel} (± 2 °C) (pure)[c]	T_{gel} (± 2 °C) (doped)[d]	Aeration coef. (s^{-1})[e]	Conversion (%)[f]	Rate constant k_{obs} ($\times 10^{-3}$ min^{-1})
1	**3**	H_2O	119 ± 39	81 ± 64	0.64 ± 0.33	34	31	0.041	83	17.3 ± 0.07
2	**4**	H_2O	2471 ± 338	192 ± 31	0.08 ± 0.03	51	43	0.066	90	20.8 ± 0.49
3	**3** + **4**[g]	H_2O	1549 ± 46	245 ± 48	0.16 ± 0.04	38	36	0.069	96	28.2 ± 2.76
4	**5**	H_2O	166 ± 31	6 ± 3	0.04 ± 0.02	53	46	0.029	76	12.3 ± 0.42
5	**6**	H_2O–DMSO[j]	11 020 ± 1483	1494 ± 231	0.14 ± 0.04	72	42	0.047	23	2.7 ± 0.21
6	**7**	CH_3CN	26 229 ± 868	5207 ± 1180	0.20 ± 0.04	80	72	0.093	100	72.6 ± 8.34
7	**8**	H_2O	162 927 ± 8676	72 969 ± 511	0.45 ± 0.02	57	53	0.051	70	11.0 ± 0.07
8	**9**	H_2O	329 206 ± 22 091	82 532 ± 14 033	0.14 ± 0.01	91	78	0.066	69	11.5 ± 0.57
9	**10**	0.5 M NaCl	28 995 ± 1371	2809 ± 151	0.12 ± 0.03	98	93	0.034	14	0.5 ± 0.07
10	**11**	PBS[k]	293 ± 24	240 ± 2	0.85 ± 0.03	56	47	0.050	55	7.3 ± 0.07
11	**12**	H_2O–AcOH[l]	235 ± 21	85 ± 21	0.36 ± 0.06	64	53	0.065	100	19.7 ± 0.64
12	**15** + **11**[h]	PBS[k]	196 ± 61	160 ± 47	0.82 ± 0.01	56	49	0.057	54	18.7 ± 0.07
13	**RFT** + **16**[i]	H_2O	21 803 ± 4052	1734 ± 7	0.08 ± 0.02	92	79	0.052	63	13.4 ± 1.48

[a] See ESI for additional information. [b] Average values calculated from randomized DTS (dynamic time sweep) experiments carried out within the linear viscoelastic regime as defined by DFS (dynamic frequency sweep) and DSS (dynamic strain sweep) measurements. *Conditions*: Frequency = 1 Hz, strain = 0.1%, temperature = 25 °C. [c] Gels prepared in the absence of a substrate and a catalyst, using the gelator concentration shown in Table 2. [d] Concentration values: Substrate **1** (doped gels) = 5.0 mmol L^{-1}, **RFT** catalyst (doped gels) = 10 mol%, total solvent volume = 1 mL, and gelator concentration as defined in Table 2. Irradiation time = 120 min, except for the organogel made in CH_3CN (entry 6) that was 60 min. All T_{gel} values were determined by IFM. [e] The aeration coefficient was determined using the dissolved oxygen microelectrode at $T = 23 \pm 1$ °C and a constant air flow rate at 0.06 bar. Estimated error = $\pm 3 \times 10^{-3}$ s^{-1}. Note that this coefficient does not represent a measurement for the reaction rate within the bulk material. [f] *Reaction conditions*: Light source = LED blue visible light (λ_{max} = 440 nm, 3 W); $T = 20 \pm 1$ °C. Reaction conversion over time for kinetics calculations was determined by ^{1}H NMR analysis. Estimated error = ±1.5%. [g] Weight ratio = 1 : 1. [h] Molar ratio of gelator system [**15** : **11**] = 1 : 96.5. [i] Molar ratio of gelator system [**RFT** : **16**] = 1 : 1. [j] Volume ratio = 95/5. [k] Phosphate buffer solution, pH 7.5. [l] Volume ratio = 80/20.

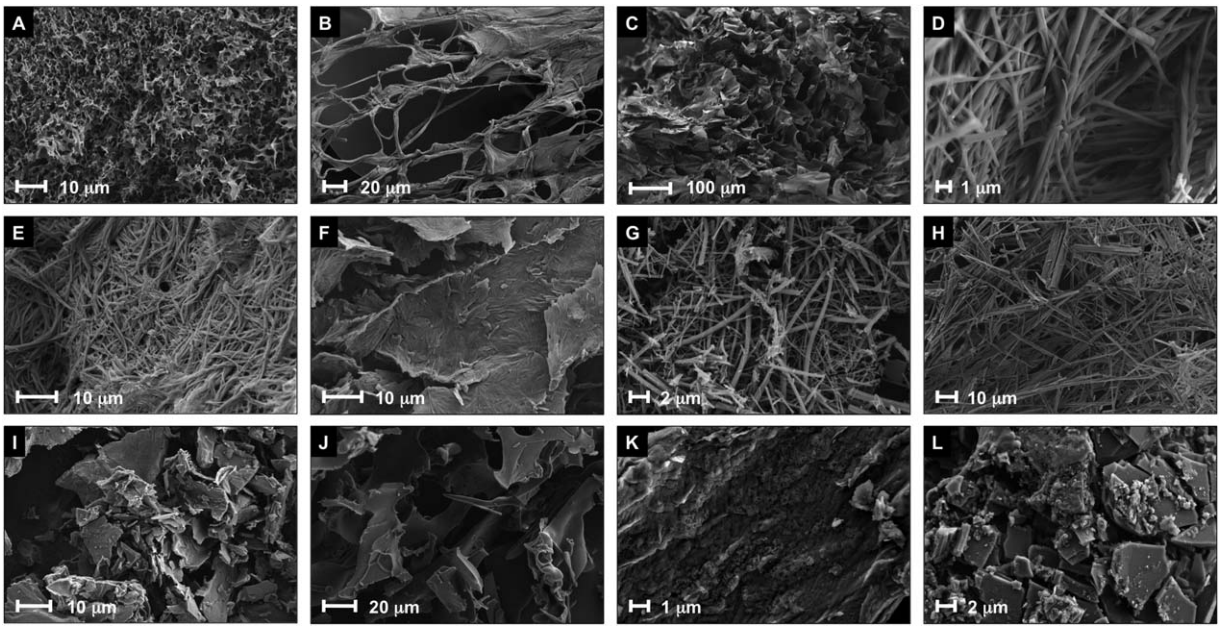

Fig. 7 Selected FESEM images of xerogels prepared by the freeze-drying method from the corresponding doped gels (*i.e.*, prepared in the presence of the substrate/catalyst under optimized conditions as described in Table 2). Gelator concentrations are given in parentheses: (A) xerogel made of **3** (5% w/v); (B) xerogel made of **4** (2% w/v); (C) xerogel made of **5** (1.5% w/v); (D) xerogel made of **6** (0.3% w/v); (E) xerogel made of **7** (0.5% w/v); (F) xerogel made of **8** (3% w/v); (G) xerogel made of **9** (3% w/v); (H) xerogel made of **10** (2% w/v); (I) xerogel made of **11** (2% w/v); (J) xerogel made of **12** (2% w/v); (K) xerogel made of [**15** + **11**] (2% w/v); (L) xerogel made of [**RFT** + **16**] (3.5% w/v). See ESI† for additional images of both pure and doped gels.

fibrillar networks were in general associated with lower reaction rates in the case of LMW hydrogels ($k_{obs} < 0.005$ min^{-1}; *e.g.*, Fig. 7d and h), whereas extended or wrinkled laminated structures with visible porosity or secondary clusters seemed to favor the reaction in both LMW and polymer gels (0.005 min$^{-1} < k_{obs} < 0.03$ min^{-1}; *e.g.*, Fig. 7a, c, f and j–l). The only exceptions to the rule were the fastest kinetics observed in the densely packed fibrillar organogel made of **7** (Fig. 7e) and the relatively slow reaction in the hydrogel made of **11** in PBS (Fig. 7i). Nevertheless, one should be very prudent regarding specific conclusions based on SEM images, as solvation in the gel phase may modify the structural packing in comparison with the dried state.[21,52]

Finally, although material rigidity could not be directly associated with product yield, the lower conversions were obtained in LMW gels of relatively high strength (*e.g.*, Table 3, entries 5 and 9). However, contrasting results obtained with other LMW and polymer gels (*e.g.*, Table 3, entries 1, 8, and 11) suggested the influence of more complex variables connected to the diffusion of reagents and/or excimer formation. Indeed, a reasonably good correlation was found between reaction rates and the aeration efficiency of most of the gels before saturation. This may be in agreement with better availability of O_2 molecules for the photocatalytic cycle inside the materials. This trend was typically observed for both LMW and polymer gels when they were considered separately, suggesting a multivariate dependence of the aeration phenomenon. Thus, an increase in the aeration efficiency was generally accompanied by an increment, albeit not proportionally, in both conversion and the reaction rate.[28]

4 Summary and conclusions

The foregoing results demonstrated that both micellar and soft gel media, including LMW and biopolymer-based gels, may serve as tunable reaction vessels for the **RFT**-catalyzed aerobic photooxidation of 1-(4-methoxyphenyl)ethanol (**1**) under LED blue visible light irradiation ($\lambda_{max} = 440$ nm). Photooxidation rates of **1** in hydrogel media were on average 10–20-fold lower than those in stirred solutions, but only 1–3-fold lower under non-stirred conditions. Moreover, the gelators could be recycled without detriment to their gelation ability and reaction conversion. Detailed kinetics studies confirmed first-order rates and the possibility of fine-tuning according to the characteristics of the confined media. In general, physical entrapment of both the catalyst and the substrate under optimized concentrations into various hydrogel matrices (approach I) permitted reaction conversions between 55 and 100% within 120 min (TOF ~ 0.045–0.08 min^{-1}), albeit with kinetics rates *ca.* 1–3-fold lower than in solution under equivalent non-stirred conditions. Remarkably, in contrast to the reaction in CH_3CN solution, the fibrillar organogel medium made of bisamide gelator **7** not only prevented photodegradation of the catalyst but also afforded full conversion in less than 60 min (TOF ~ 0.167 min^{-1}; $k_{obs} \sim 0.073$ min^{-1}) without the need of thiourea. Other strategies (approaches II and III) based on a higher degree of organization of the catalyst within the gel network led to slower reaction rates in comparison with the first approach. In addition, despite the presence of a chiral environment (approaches I and II) both substrate enantiomers were equally oxidized, suggesting the absence of selective interactions with the fibrillar gel structure.

Although no unambiguous associations could be made between reaction kinetics and morphology of the gels, the former was generally in good agreement with the relative aeration efficiency of the gel media.

This study constitutes one of the few reports so far dealing with photochemical reactions inside gels. The comprehensive kinetics analyses and the demonstrated influence of the local environment may help to design new gel materials as biomimetic nanoreactors for photochemical transformations.

Acknowledgements

We thank CSIC (PIE 200980I059), Univ. Regensburg (Förderlinie C des Finanziellen Anreizsystems für Drittmitteleinwerbung), Ministerio de Ciencia e Innovación-FEDER (CTQ2010-17436; J.B., predoctoral fellowship), Gobierno de Aragón-FSE (research group E40), the German Academic Exchange Service (DAAD, INDIGO program) and the German Science Foundation (DFG, GRK 1626 Chemical Photocatalysis) for financial support. We are indebted to Prof. A. Göpferich for assistance with rheological measurements. B.B.D. thanks CSIR for a Senior Research Associateship (Scientists' Pool Scheme). D.D.D. thanks Professors M.G. Finn and V. Rodionov for helpful discussions.

Notes and references

1 D. M. Vriezema, M. C. Aragonés, J. A. A. W. Elemans, J. J. L. M. Cornelissen, A. E. Rowan and R. J. M. Nolte, *Chem. Rev.*, 2005, **105**, 1445–1489.
2 S. A. Bode, I. J. Minten, R. J. M. Nolte and J. J. L. M. Cornelissen, *Nanoscale*, 2011, **3**, 2376–2389.
3 L. Marchetti and M. Levine, *ACS Catal.*, 2011, **1**, 1090–1118.
4 J. Rebek, *Acc. Chem. Res.*, 2009, **42**, 1660–1668.
5 B. Breiner, J. K. Clegg and J. R. Nitschke, *Chem. Sci.*, 2011, **2**, 51–56.
6 V. Ramamurthy and A. Parthasarathy, *Isr. J. Chem.*, 2011, **51**, 817–829.
7 M. Yoshizawa, J. Klosterman and M. Fujita, *Angew. Chem., Int. Ed.*, 2009, **48**, 3418–3438.
8 Y. Inokuma, M. Kawano and M. Fujita, *Nat. Chem.*, 2011, **3**, 349–358.
9 R. K. O'Reilly, *Philos. Trans. R. Soc. London, Ser. A*, 2007, **365**, 2863–2878.
10 A. Ostafin and Y.-C. Chen, in *Kirk-Othmer Encyclopedia of Chemical Technology*, John Wiley and Sons, 2009, pp. 1–18.
11 For selected examples, see: A. Maldotti, A. Molinari and R. Amadelli, *Chem. Rev.*, 2002, **102**, 3811–3836; D. G. Shchukin and D. V. Sviridov, *J. Photochem. Photobiol., C*, 2006, **7**, 23–39; J. Matsumoto, T. Matsumoto, Y. Senda, T. Shiragami and M. Yasuda, *J. Photochem. Photobiol., A*, 2008, **197**, 101–109; C. Harris and P. V. Kamat, *ACS Nano*, 2009, **3**, 682–690; B. Cojocaru, S. Neatu, V. I. Parvulescu, K. Dumbuya, H.-P. Steinrück, J. M. Gottfried, C. Aprile, H. Garcia and J. C. Scaiano, *Phys. Chem. Chem. Phys.*, 2009, **11**, 5569–5577; F. A. Leibfarth, K. M. Mattson, B. P. Fors, H. A. Collins and C. J. Hawker, *Angew. Chem., Int. Ed.*, 2013, **52**, 199–210.
12 For selected reviews on gel materials and applications, see: L. A. Estroff and A. D. Hamilton, *Chem. Rev.*, 2004, **104**, 1201–1218; N. M. Sangeetha and U. Maitra, *Chem. Soc. Rev.*, 2005, **34**, 821–836; P. Xie and R. Zhang, *J. Mater. Chem.*, 2005, **15**, 2529–2550; M. George and R. G. Weiss, *Acc. Chem. Res.*, 2006, **39**, 489–497; G. C. Maity, *J. Phys. Sci.*, 2007, **11**, 156–171; R. V. Ulijn and A. M. Smith, *Chem. Soc. Rev.*, 2008, **37**, 664–675; A. R. Hirst, B. Escuder, J. F. Miravet and D. K. Smith, *Angew. Chem., Int. Ed.*, 2008, **47**, 8002–8018; S. Banerjee, R. K. Das and U. Maitra, *J. Mater. Chem.*, 2009, **19**, 6649–6687; M. O. M. Piepenbrock, G. O. Lloyd, N. Clarke and J. W. Steed, *Chem. Rev.*, 2010, **110**, 1960–2004; D. J. Adams, *Macromol. Biosci.*, 2011, **11**, 160–173; A. Dawn, T. Shiraki, S. Haraguchi, S. Tamaru and S. Shinkai, *Chem.–Asian J.*, 2011, **6**, 266–282; X. Yang, G. Zhang and D. Zhang, *J. Mater. Chem.*, 2012, **22**, 38–50; A. Noro, M. Hayashi and Y. Matsushita, *Soft Matter*, 2012, **8**, 2416–2429.
13 D. D. Díaz, D. Kühbeck and R. J. Koopmans, *Chem. Soc. Rev.*, 2011, **40**, 427–448, and references therein; A. Shumburo and M. C. Biewer, *Chem. Mater.*, 2002, **14**, 3745–3750.
14 M. Pagliaro, R. Ciriminna and G. Palmisano, *Chem. Soc. Rev.*, 2007, **36**, 932–940; F. Rodríguez-Llansola, J. Miravet and B. Escuder, *Chem.–Eur. J.*, 2010, **16**, 8480–8486; P. D. Wadhavane, M. A. Izquierdo, F. Galindo, M. I. Burguete and S. V. Luis, *Soft Matter*, 2012, **8**, 4373–4381.
15 There is vast literature dealing with photoresponsive moieties covalently incorporated in gelator structures for tuning either the *sol*-to-*gel* phase transition or the mechanical robustness of the material upon light-induced isomerization or polymerization reactions. For representative examples, see those collected in ref. 13
16 S. Bhat and U. Maitra, *Molecules*, 2007, **12**, 2181–2189.
17 A. Dawn, N. Fujita, S. Haraguchi, K. Sada and S. Shinkai, *Chem. Commun.*, 2009, 2100–2102; A. Dawn, N. Fujita, S. Haraguchi, K. Sada, S.-i. Tamaru and S. Shinkai, *Org. Biomol. Chem.*, 2009, **7**, 4378–4385.
18 For selected examples of light-harvesting studies in hybrid non-covalent assemblies, see: M. Kercher, B. König, H. Zieg and L. De Cola, *J. Am. Chem. Soc.*, 2002, **124**, 11541–11551; H. F. M. Nelissen, M. Kercher, L. De Cola, M. C. Feiters and R. J. M. Nolte, *Chem.–Eur. J.*, 2002, **8**, 5407–5414; M. Braun, S. Atalick, D. M. Guldi, H. Lanig, M. Brettreich, S. Burghardt, M. Hatzimarinaki, E. Ravanelli, M. Prato, R. van Eldik and A. Hirsch, *Chem.–Eur. J.*, 2003, **9**, 3867–3875; B. Ferrer, G. Rogez, A. Credi, R. Ballardini, M. T. Gandolfi, V. Balzani, Y. Liu, H.-R. Tseng and J. F. Stoddart, *Proc. Natl. Acad. Sci. U. S. A.*, 2006, **103**, 18411–18416; K. V. Rao, K. K. R. Datta, M. Eswaramoorthy and S. J. George, *Chem.–Eur. J.*, 2012, **18**, 2184–2194, and references therein.
19 K. V. Rao, K. K. R. Datta, M. Eswaramoorthy and S. J. George, *Angew. Chem., Int. Ed.*, 2011, **50**, 1179–1184.
20 P. Jana, S. Maity, S. K. Maity, P. K. Ghorai and D. Haldar, *Soft Matter*, 2012, **8**, 5621–5628.
21 S. Samai, P. Ghosh and K. Biradha, *Chem. Commun.*, 2013, DOI: 10.1039/c2cc34901a.

22 G. H. Pollack, *Cells, Gels and the Engines of Life: A New, Unifying Approach to Cell Function*, Ebner & Sons, Seattle WA, USA, 2001.
23 B. Rybtchinski, *ACS Nano*, 2011, **5**, 6791–6818.
24 J. N. Hunt, K. E. Feldman, N. A. Lynd, J. Deek, L. M. Campos, J. M. Spruell, B. M. Hernandez, E. J. Kramer and C. J. Hawker, *Adv. Mater.*, 2011, **23**, 2327–2331.
25 Additional saturation with O_2 has been proven to quench the flavin excited state, see: H. Schmaderer, P. Hilgers, R. Lechner and B. König, *Adv. Synth. Catal.*, 2009, **351**, 163–174.
26 J. Svoboda, H. Schmaderer and B. König, *Chem.–Eur. J.*, 2008, **14**, 1854–1865.
27 For the study of other photochemical reactions in micellar solutions of NaDC, see: M. Pattabiraman, L. S. Kaanumalle and V. Ramamurthy, *Langmuir*, 2006, **22**, 2185–2192.
28 See ESI for details.†
29 V. Massey, *Biochem. Soc. Trans.*, 2000, **28**, 283–296, and references therein.
30 Y. Imada, T. Kitagawa, T. Ohno, H. Iida and T. Naota, *Org. Lett.*, 2010, **12**, 32–35, and references therein.
31 R. Lechner, S. Kümmel and B. König, *Photochem. Photobiol. Sci.*, 2010, **9**, 1367–1377, and references therein.
32 J. F. Teichert, T. den Hartog, M. Hanstein, C. Smit, B. ter Horst, V. Hernandez-Olmos, B. L. Feringa and A. J. Minnaard, *ACS Catal.*, 2011, **1**, 309–315.
33 Y. Imada, H. Iida, T. Kitagawa and T. Naota, *Chem.–Eur. J.*, 2011, **17**, 5908–5920.
34 J. Dad'ová, E. Svobodová, M. Sikorski, B. König and R. Cibulka, *ChemCatChem*, 2012, **4**, 620–623.
35 R. Lechner and B. König, *Synthesis*, 2010, **10**, 1712–1718.
36 W. A. Massad, Y. Barbieri, M. Romero and N. A. Garcia, *Photochem. Photobiol.*, 2008, **84**, 1201–1208.
37 O. Lu, G. Bucher and W. Sander, *ChemPhysChem*, 2004, **5**, 47–56.
38 R. Cibulka, R. Vasold and B. König, *Chem.–Eur. J.*, 2004, **10**, 6223–6231, and references therein.
39 For a detailed mechanistic study, see: U. Megerle, M. Wenninger, R.-J. Kutta, R. Lechner, B. König, B. Dick and E. Riedle, *Phys. Chem. Chem. Phys.*, 2011, **13**, 8869–8880.
40 Although the data of a few examples suggested a complex kinetic in nature (see ESI†), first-order assumptions provided the best fit in each case. For our experiments in air, and from a mechanistic point of view, this was also consistent with an O_2 concentration well above the saturating concentration for the reaction with the excited state of the sensitizer.
41 In general, photooxidation of benzyl alcohols in aqueous and acetonitrile solutions yields the corresponding aldehydes as the sole product. However, traces of benzoic acids have been occasionally observed with immobilized flavins due to overoxidation (see ref. 24).
42 M. Pattabiraman, L. S. Kaanumalle and V. Ramamurthy, *Langmuir*, 2006, **22**, 2185–2192.
43 M. Marchena and F. Sanchez, *Prog. React. Kinet. Mech.*, 2010, **35**, 27–80.
44 H. Svobodová, V. Noponen, E. Kolehmainen and E. Sievänen, *RSC Adv.*, 2012, **2**, 4985–5007.
45 H. Koshima, W. Matsusaka and H. Yu, *J. Photochem. Photobiol., A*, 2003, **156**, 83–90.
46 M. I. Burguete, M. A. Izquierdo, F. Galindo and S. V. Luis, *Chem. Phys. Lett.*, 2008, **460**, 503–506, and references therein.
47 J. Svoboda and B. König, *Chem. Rev.*, 2006, **106**, 5413–5430.
48 For the use of chiral host molecules for enantioselective photoreactions via chirality transfer, see for example: P. Selig and T. Bach, *J. Org. Chem.*, 2006, **71**, 5662–5673, and references therein.
49 Molecular aggregation has also been found to play an important role in some catalytic processes dealing with chirality amplification; see for example: D. G. Blackmond and M. Klussmann, *Chem. Commun.*, 2007, 3990–3996.
50 Detailed photodegradation studies of riboflavin derivatives have been carried out under different conditions. For selected examples, see: I. Ahmad, Q. Fasihullah and F. H. M. Vaid, *Photochem. Photobiol. Sci.*, 2006, **5**, 680–685, and references therein; I. Ahmad, Q. Fasihullah and F. H. M. Vaid, *J. Photochem. Photobiol., B*, 2006, **82**, 21–27; H. Görner, *J. Photochem. Photobiol., B*, 2007, **87**, 73–80; I. Ahmad, S. Ahmed, M. A. Sheraz and F. H. M. Vaid, *J. Photochem. Photobiol., B*, 2008, **93**, 82–87; I. Ahmad, S. Ahmed, M. A. Sheraz, F. H. M. Vaid and I. A. Ansari, *Int. J. Pharm.*, 2010, **390**, 174–182; M. Insinska-Rak, A. Golczak and M. Sikorski, *J. Phys. Chem. A*, 2012, **116**, 1199–1207.
51 A. Saha, B. Roy, A. Esterrani and A. K. Nandi, *Org. Biomol. Chem.*, 2011, **9**, 770–776.
52 K. A. Houston, K. L. Morris, L. Chen, M. Schmidtmann, J. T. A. Jones, L. C. Serpell, G. O. Lloyd and D. J. Adams, *Langmuir*, 2012, **28**, 9797–9806.

